

Supplemental Figure Legends

Figure 1: A: Quantification of signal intensities obtained by Northern on total RNA isolated from fetal heart (E16), and 4 and 7 days (4d, 7d) after birth. The data is normalized with the signal obtained with U6. Representative radiograms are shown in Figure 1B of the manuscript. Each bar is a mean of a minimum of n=4. Significant ($p<0.05$) * when compared to fetal heart, # when compared to 4d neonatal heart. B. Relative distribution of miR-378 in various tissues of adult mice as analyzed by Northern (n=2). Representative radiograms are shown in Figure 1D of the manuscript.

Figure 2: Predicted secondary structure of the miR-378-IGF1R-3'UTR target duplex using a software RNAhybrid (bibiserv.techfak.uni-bielefeld.de/rnahybrid) showing base pairings of duplex between miR-378 and wild type IGF1R 3'UTR target (on left) or mutant target nucleotides (on right) used in the luciferase functional assays. The functional data of this assay is presented in Figure 4D of the manuscript. Note incorporation of mutations in the seed base-pairing region of target significantly increased the minimum free energy (mfe) of the mutant duplex affecting binding of miR-378 (shown in green) with the mutant IGF1R (shown in red), the 5' end of each molecule is also marked.

Figure 3: Combined effect of IGF1R inhibitor and PI3K inhibitor on IGF-induced AKT activation in mock control, mimic control or 378-mimic transfected cardiomyocytes. Note over-expression of miR-378 enhanced IGF1R and PI3K inhibition on IGF1 induced AKT activation in cardiomyocytes, suggesting involvement miR-378 in IGF1R-mediated signaling cascade. Data is presented as mean \pm SD of n=2. Significant ($p<0.05$) *when compared to corresponding non-treated group, # when compared to similarly treated either mock or mimic control groups.

Figure 4: Representative confocal images of TUNEL stained cardiomyocytes. Cells were transfected with either scramble control or 378-antimiR, after 48 h cells were exposed to various periods of hypoxia and reoxygenation periods as indicated on left. To-Pro stained nuclei (blue), TUNEL stained fragmented DNA (green) and two images merged together are shown. Quantification of the data is presented in Figure 8C of the manuscript.

Figure 5: Representative immunofluorescence images of cardiomyocytes used for quantification TUNEL positive nuclei in Figure 8D of the manuscript. To-Pro stained nuclei (blue), fragmented DNA TUNEL stained nuclei (green) and two images merged together in different treatment groups as indicated on left are shown.

Figure 6: Quantification of IGF1 expression in fetal heart and after birth at indicated age in weeks (wk) and in cultured cardiac fibroblasts derived from the neonatal rat heart. Data is normalized for β -actin expression obtained in the same blot. Representative image is presented in Figure 9B of the manuscript. Significant ($p<0.05$) compared to 16 d fetal heart.

Supplemental Figure 1A:

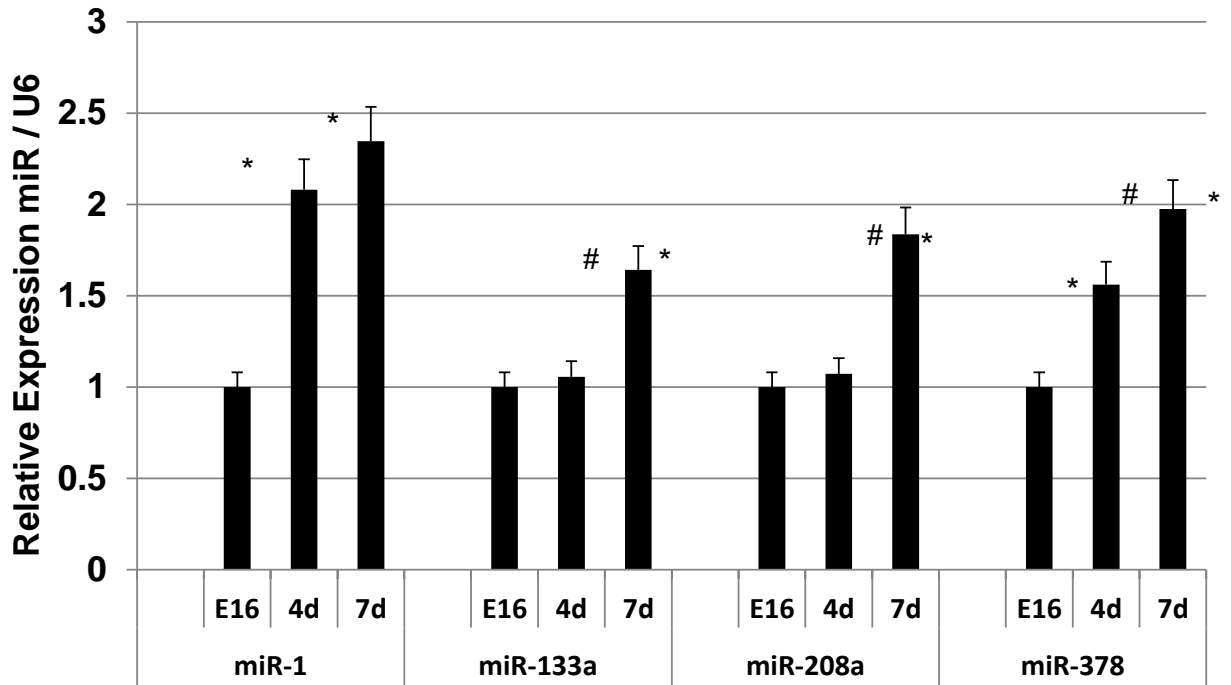


Figure 1B:

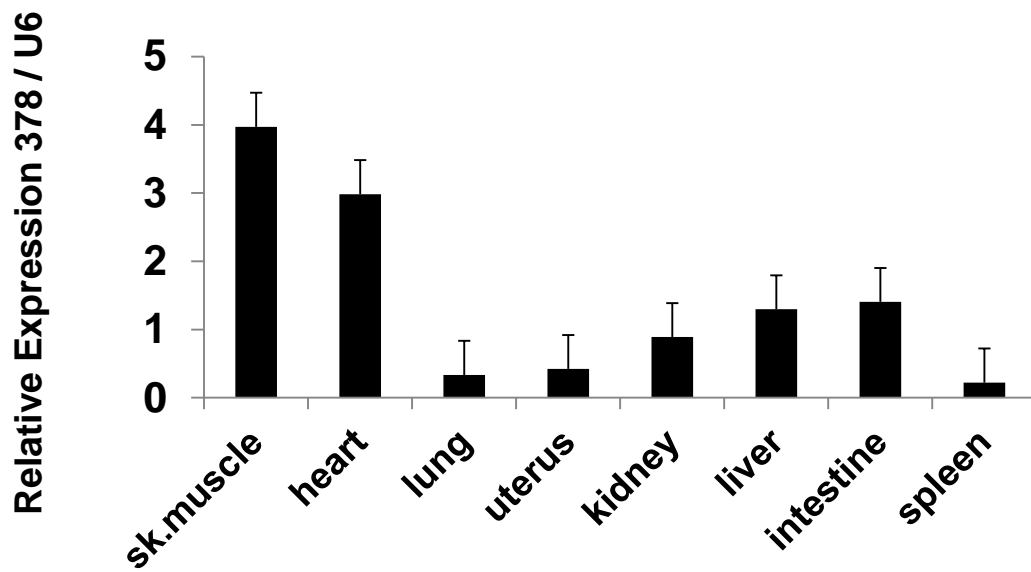


Figure 2:

Wt IGF1R3X-Luc AATAGGGCTCTTAAGTCCAGTA

Mut IGF1R3X-Luc AACAGGCCTCTTACATGATCTA

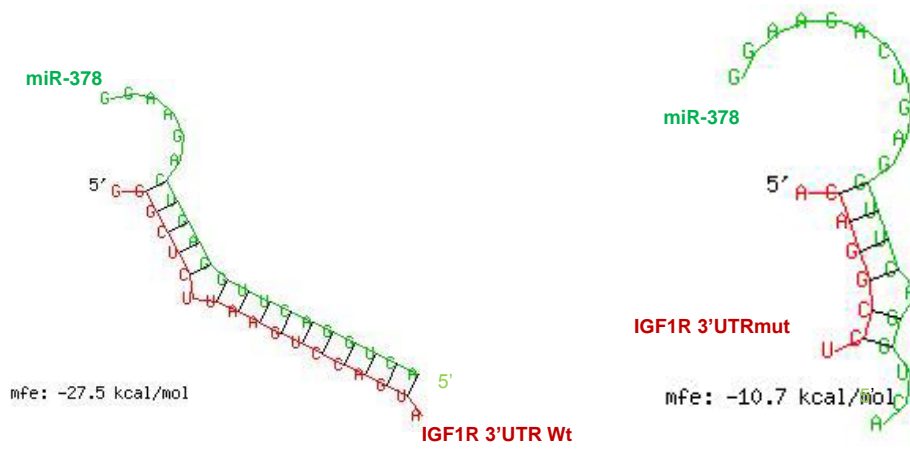


Figure 3

Mimic control 10 nM	-	-	-	-	+	+
378-mimic 10nM	-	-	+	+	-	-
PQ-410 5uM	-	+	-	+	-	+
LY294002 1uM	-	+	-	+	-	+

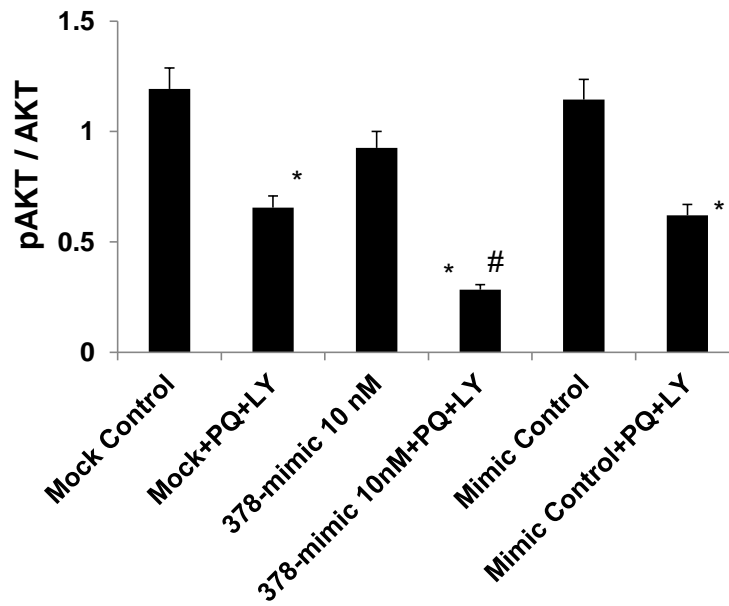
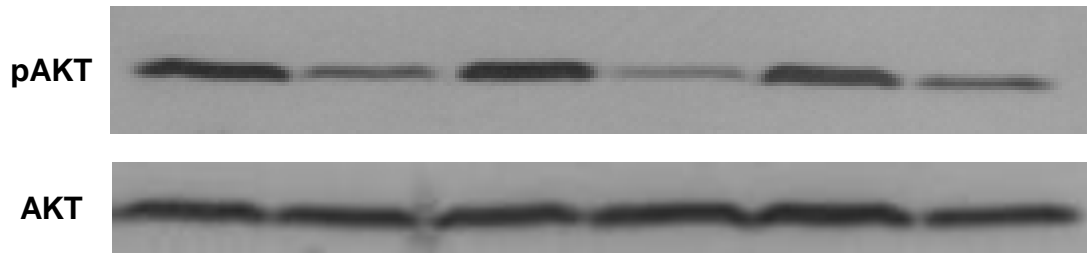


Figure 4:

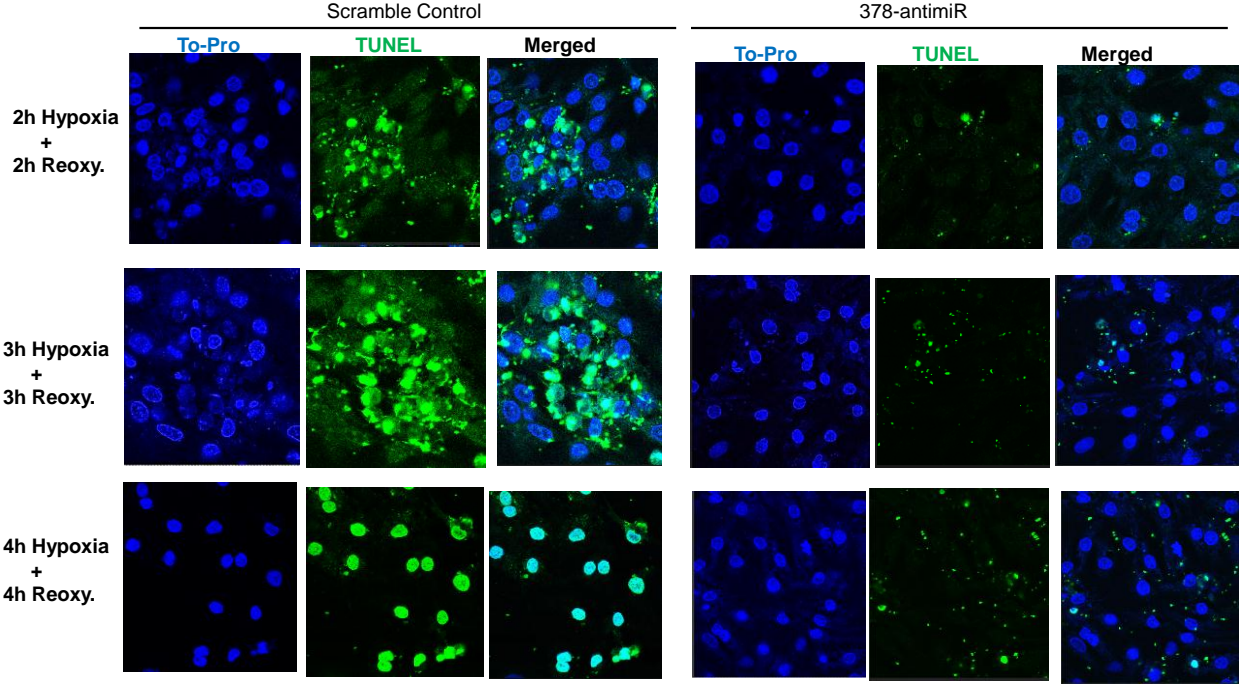


Figure 5

2h Hypoxia + 2h Reoxygenation

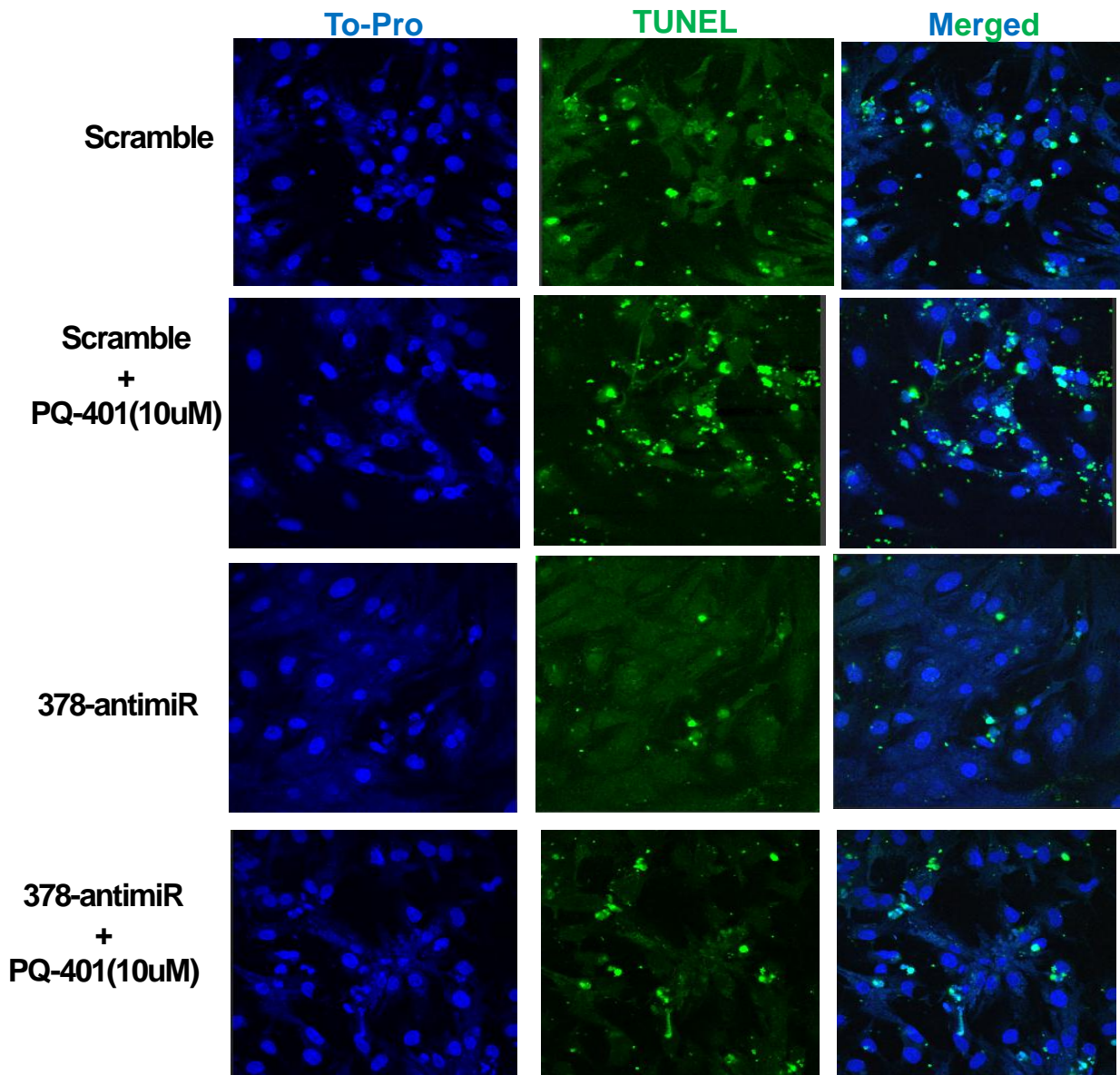


Figure 6:

